The Korean Journal of Rheology,
Vol. 2, No. 2, December 1990, pp.7-18

〈총설〉

원형 Film Blowing 공정의 모델링

서용석 · 김광웅

한국과학기술연구원 고분자 공정연구실

(1990년 12월 26일 접수)

Modeling of Tubular Film Blowing Process

Yongsok Seo and Kwang Ung Kim

Polymer Processing Laboratory KIST, P.O. Box 131 Cheongryang, Seoul Korea

(Received December 26, 1990)

Introduction

Film blowing process is used for the manufacture of a thin sheet or film of a thermoplastic material (e.g. polyethylene, polypropylene, polystyrene) from molten polymer supplied under pressue by a screw extruder. The polymer melt is forced through an annular die and the tubular film so formed is thinned both by blowing and axial drawing. The tube is formed into a cloed bubble by flattening it when it is cooled enough to avoid blocking (the tendency of the film to stick to itself) and then the flattened film is wound onto takeup rolls. The axial tension is provided by the driven nip rolls which close the bubble at the top (the process is usually run vertically with the die at the bottom). The blowing is caused by manintaining an air pressure slightly above atmospheric pressure inside the bubble and this causes the increase of the parison radius and stretching of the film in a circumferential direction. When the bubble reaches at freezing line, the parison gets a constant radius. Fig. 1 shematically illustrates the process.

The development of molecular orientation and consequently the physical and mechanical properties (e.g. tensile strength, tear strength, gas permeabliity, clarity, resistance to crazing) are greatly influenced by deformation and thermal histories of the material. From the processing point of view, the tubular film blowing process has been gaining importance in industry because it provides biaxially oriented thin film via single step.

The film blowing process has been studied from many different points of view. Intensive efforts were invested in the film blowing process simulation. The purpose of the modeling of blwon film process is to develop a method for procicting the physical properties of the formed film to improve the efficiency of resin and process development without making blown film from literally tons of experimental resin to determine the effect of process parameters on film properties. In this article, we summarize the current status of film blowing process modeling and suggest future works.

Process Analysis

From the rheological point of view, the film blowing process can be divided into three zones, a) die extrusion region b) blowing region c) the region over the frost line. We briefly overview these separately.

A) Die Extrusion Region

The polymer melts are extruded through annular die and extrudate will be swollen (This is well kown "extrudate swell" phenomenon) with cooling on both inside and outside surfaces by cooling air. Since the extrudate swell affects film dimensions and accordingly all physical, rheological and optical properties of the film, it should be included in the analysis of film blowing process. Extrudate swell prediction is not a simple work and it is a real horror of peoples working in computational fluid mechanics field due to difficulty of so-called high Weissenberg number problem. Extrudate swell phenomena have been intensively studied numerically using a finite elemt mehtod. As well known [1], the cause of extrudate swell is very complicated. In the present problem, one now sees four major contributions to extrudate swell, that is,

(1) Elastic strain recovery
(2) Inelastic Newtonian swelling
(3) Inelastic thermal swelling
(4) The effect of branching and molecular weight distribution.

Needless to say, the elastic strain recovery is the most important factor among these. With the assumption of incompressible fluid, continuity equation, momentum equation, energy equation can be solved together with numerous constitutive equations by either a finite element method (FEM) or a finite difference method (FDM) [2]. In these days, FEM is prevalently used for extrudate swell analysis. For Newtonian fluids or inelastic viscous fluids, swell prediction is relatively easy in spite of many times of interation for the free surface position. Inelastic thermal swelling problem can be also easily handled. The probelm occurs with the adoption of a constitutive equation for the viscoelastic fluid. Lots of different constitutive equations with many different numerical techniques were tried to solve the extrudate swell problem for highly elastic fluids (so called high Weissenberg number problem) [2]. Unfortunately, nearly all of thse constitutive equations based on continuum mechanics could not overcome the limit of high Weissenberg number or Deboah number. This is due to the nature of constitutive equations nonlinearity which is unavoidable. Rencetly there was a report that high Weissenberg number problem could be solved using the constitutive equation originated from the molecular concept (Curtiss-Bird model). This problem is still on the hot plate waiting for more stable algorithm with more sound and easily controllable constitutive equation.

For annular extrudate outcoming from an annular die used in film blowing process, one more nonlinearity exists compared to capillary or plane extrudates, that is, it has two free surfaces which needs more computional time. For inelastic fluids, it does not add any difficulties at all. Annular extrudate swell phenomena were investigated for inelastic fluids andd viscoelastic fluids using FEM [3-7]. These studies include the effect of many different factors such as Newtionian fluids, inelastic Non-Newtonian fluids, different die geometry effect, thermal swelling with heat convection, second-order fluid, elastic fluid following Maxwell model. Gravitational force and surface tension effects are also studied.

As mentioned above, since extrudate swell affects the final product dimension, it is quite important in the simulation of film blowing process. The was investigated recently be Seo and Wissler [8]. However, their study was limited to a Newtonian fluid case. Even for a Newtonian fluid, swelling exhibited a remarkable difference when it was included and excluded in the simulation. Details about this are discussed below.

B) Blowing Region

Blowing process is generally started by capping on annular extrudate and sealing the formed bubble with the nip rolls. Air is then introduced into the bubble and nip rolls and the extruder are increased in speed until the process requirements are met. The polymer is stretched up to the freeze line and then the frozen-in-strain partially relaxes as the polymer continues to cool between the freeze line and the nips. Freezing line is a kinematic constant on the film blowing process as defined by Pearson and Petrie [9]. It is the point

where the film is parallel to the center line of the bubble, which more or less corresponds to the obscured frost line. However, frost line position is related with crystallization of which height are influenced by the velocity and temperature of the air that is applied to the exterior of the bubble by one or more annular jets produced by an air ring. The refractive index of the polymer changes rapidly at the frost line (Fig. 1).

Generally blowing region is defined as the distance between the die exit and freeze line. Clegg and Huck [10] investigated the film properties related to key processing variables in an experimental manner. Holmes *et al.* [11] proposed a mathematical model for the heat tansfer process in film blowing process while Ast [12, 13] measured the temperature profiles for low density polyethylene films and Predoehl [14] considered heat radiation effect on film blowing process. Some of the stresses that existed in the polymer melts were examined by Dowd [15] and the deformation caused by these stresses was measured by Farber and Dealy [16]. The various instabilities that manifest themselves in this process has been documented by Han and Park [17]. From the theoretical point of view, is seems that Alfrey [18] was the first to set up the basis of process analysis based on membrane theory. Later Pearson and Petrie [9, 19, 20] first built a rigorous mathematical model to describe the process based on membrane theory even though they restricted the treatment to isothermal Newtonian fluids. The non-Newtonian fluid was considered later by Petrie [21] who numerically obtained bubble shapes for different Maxwell type models and extended the calculations to a nonisothermal Newtonian fluid [22]. Agreement between theoreticfal predictions and experimental measurement was sought by Wagner [24] with integral type constitutive equation (rubberlike liquid with one time constant). Wagner additionally incorporated temperature changes in the biaxial extension of the bubble. Han and Park [25] applied an elongational type equation to film blowing process. Recently Gupta and Metzner [26] used nonisothermal viscoelastic constitutive equation (modified White-Metzner equation) to superpose the fluid memory and temperature. The application of different constitutive equation and its effect on simulation are briefly presented afterwards.

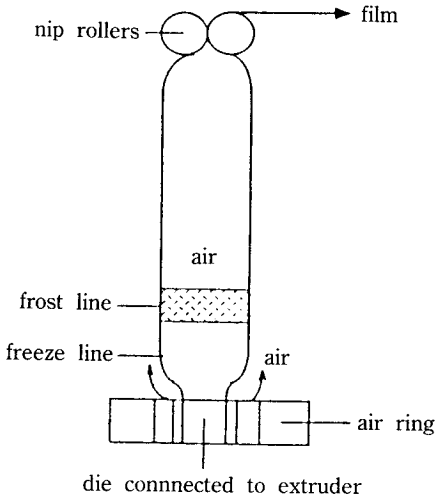

Fig. 1. Blown film line.

Following the classical pattern of Pearson and Petrie [9], the film is regarded as a thin shell in tension: the tension is supported by longitudinal traction (F_z) in the bubble and by internal air pressure (ΔP). Inertia, surface tension, air drag and gravity forces can be included even though they are generally regarded as negligible in lab scale experiments due to the thinness of the membrane and the speeds of typical operations, but full equations are easily derivable as shown later. With further assumptions of no variation across the film thickness and steady axisymmetric flow, at least until freezing sets in, the problem is conveniently handled using local Cartesian coordinates, x_1 in the direction of flow, x_2 normal to the film, and x_3 in the transverse direction. The simple force balance normal to the film (from standard membrane theory neglecting gravity, inertial, surface tension and air drag) gives

$$\frac{\Delta P}{H} = \frac{\sigma_{11}}{R_1} + \frac{\sigma_{33}}{R_3} \tag{1}$$

Where ΔP is the inflation pressure, H is the film

thickness, R_1 and R_3 are principal radil of curvature, and σ_{11} and σ_{33} are principal stresses in x_1 and x_3 directions respectively. A similar force balance in the machine direction gives.

$$F_1 = 2\pi a H \sigma_{11} \cos\theta - \pi a^2 \Delta P \tag{2}$$

Where F_1 is the applied force in the machine direction, a is the radius of the cylindrical bubble,and θ is the angle between the velocity vector (the local x_1 direction) and the center line. We take z as our coordinate in the machine direction and then straight forward geometry gives,

$$\frac{da}{dz} = \tan\theta \tag{3}$$

$$R_1 = a \sec\theta \tag{4}$$

$$R_2 = -(1+(da/dz)^{3/2})/(d^2a/dz^2) \tag{5}$$

As usually assumed in free-surface flows we take $\sigma_{22}=O$ (when surface tension is being neglected) from which following equations are obtained

$$\sigma_{11} = \tau^E_{11} - \tau^E_{12} \tag{6}$$

$$\sigma_{33} = \tau^E_{33} - \tau^E_{22} \tag{7}$$

where τ^E is the extra stress tensor.

The kinematics, which we shall need for the rheological equation of state in order to obtain τ^E, are those of elongational flow, with rate of strain tensor

$$\mathbf{D} = \cos\theta \begin{bmatrix} dv/dz & 0 & 0 \\ 0 & (v/a)(da/dz) & 0 \\ 0 & 0 & (v/a)(dH/dz) \end{bmatrix} \tag{8}$$

where we write v for the velocity (in the x_1-direction), and defromation tensor

$$\mathbf{C}^{-1} = \begin{bmatrix} v^2/v_0^2 & 0 & 0 \\ 0 & a^2/a_0^2 & 0 \\ 0 & 0 & H^2/H_0^2 \end{bmatrix} \tag{9}$$

relative to the initial state of the material (at $z=O$, after allowing for the extrudate swell if necessary). For an incompressible material we have the constraint that the trace of **D** is zero (in isothermal flow) and more generally, allowing the density to vary with temperature and hence with position in the more realistic non-isothermal situation, we have

$$\dot{M} = 2\pi\rho a \, Hv \tag{10}$$

where $\dot{M}$ is the mass flow rate which is constant for steady flow.

A constitutive equation, to relate τ^E to **D** or $\mathbf{C}^{-1}$ or some function of the history of these quantities makes the set of equations for the dynamics. The choice of constitutive equation affects the mathematical structure of the model. Here we note that this has an effect on the number and type of boundary conditions requried at die exit ($z=O$). The complete model of dynamics requires knowledge of initial values of a, H and v and the value of θ at the freeze-line. Incorporation of other forces merely requires alteration of equations to a more realitic mechanical equations.

$$\Delta P_2 + \rho g H \sin\theta = \frac{H(\sigma_{11}-\rho v^2)+2\sigma_s}{R_1} + \frac{H\sigma_{22}+2\sigma_s}{R_2} \tag{11}$$

$$F_1 = 2\pi a[H(\sigma_{11}-\rho v^2)+2\sigma_s] \cos\theta - \pi a^2 \Delta P \tag{12}$$

$$\frac{dF}{dz} = 2\pi a(T_{drag} + \rho g H/\cos\theta) \tag{13}$$

Here we have allowed for gravity (the terms involving ρg), inertia (the terms involving ρv). surface tension (coefficient σ_s) and air drag (shear stress T_{drag} acting on the film in the negative x_1 direction). Completion of the model requires knowledge of the film temperature as a function of z so that density and the rheological properties of the polymer may be correctly incorporated into the computation. One crucial aspect of the freeze-line position for the geometrical and mechanical boundary conditions, involves assumptions about the freeze-line as well as the die exit region. In order to make calculations of the temperature we need to use the energy equation which may be written

$$\dot{M}\frac{d(\gamma T)}{dz} = -[\alpha(T-T_c)+\varepsilon\sigma_B(T^4-T_a^4)]\frac{2\pi a}{\cos\theta} \tag{14}$$

where T(z) is the film temperature, γ its specific

heat, T_c the temperature of the cooling air, α the appropriate heat transfer coefficient, ε the emissivity of the film of molten polymer, σ_B the Stefan-Boltzmann constant and T_a the ambient temperature. In writing eqn. (14), we ignore heat transfer into the interior of the tubular bubble. Convection inside the bubble can provide a mechanism for additional cooling of the bubble near the die. Equation for the temperature of the film allows temperature-denpendent properties to be used in the dynamic equation. The appearance of a and θ in eqn. (14) means that the solutions of the equations are coupled. Depending on the constitutive equation, different approaches can be applied to solve the dynamic equations. For a Newtonian fluid, we can change the dynamic equations into dimensionless equations. In a dimensionless form, the model system for a Newtonian fluid consists of two ordinary differential equation for the dimensionless radius r and thickness h (Pearson and Petrie [9] as functions of $x=z/a_0$.)

$$2r^2(T_1+Br^2)r''+(1+r'^2)\ (T_1-3Br^2)r \tag{15}$$

$$\frac{h'}{h}=-\frac{r'}{2r}-\frac{1}{4}(1+r'^2)(T_1+Br^2) \tag{16}$$

with boundary conditions

$$r=1,\ h=1\ \text{at}\ x=Z/a_0=0 \tag{17}$$

$$r'=0\ \text{at}\ x=X=Z_f/a_0 \tag{18}$$

where Z_f is the freeze-line height. Here r, h, B, T, are dimensionless variables defined as

$h=H/H_0$
$r=a/a_0$
$R=A/a_0$
$B=\pi\ a_0^3\ \Delta P/\eta_0 q$
$T_1=T_z\text{-}BR^2$
$T_z=a_0F_z\eta_0 q$

in which physical parameters are defined as follows

η_0=viscosity
q=the total volumetric flow rate
ΔP=the pressure difference across the bubble
F_z=axial force applied at the freeze line
A=the maximum radius of the bubble (at the freeze line)
H_0=the film thickness at the die (or die gap)
a_0=the radius of the die

The boundary condition at $X=Z_f/a_0$ arises because it is the condition at the freeze-line of the bubble that control the process; when the material freezes, since no further deformation is possible, r' must become zero at the freeze line. Using dimensionless variables the energy equation can be written.

$$Y'=-rC_h(Y-Y_L+E_s\ (Y^4-Y_s^4) \tag{19}$$

where $Y=T/T_0$, $C_h=2\pi R/MC_p$, a dimensionless heat transfer coefficient, $E_s=\varepsilon\ C_sT_0^3/C_h$ a dimensionless constant. Temperature boundary condition should be added in nonisothemal problem. The other bounary conditions at z=o should be changed if die swelling is considered, i.e., it should be changed as

$$r=r_a\ \ h=h_a\ \text{at}\ x=z'/a_0 \tag{20}$$

where r_a and h_a are radius and thickness at the end of the swelling region ($x=z'/a_0$). Equations (15), (16) and (19) can be solved empolying integration procedure such as Runge-Kutta method. For a Newtonian fluid, the integration was carried out from x=X (where r=R and r'=0) to x=0. After the calculation was done till x=0 (or $x=x_i$ for swelling case) the values of radius, thickness, and temperature at final position were compared and if they didn't agree with given boundary condition, then Δp, F_R and α were changed and the calculation was repreated to obtain the optimized values. This iteration was done using a Newton-Raphson method as follows. Define functions f_1, f_2, f_3 and variables x_1^*, x_2^*, x_3^* as follows:

$f_1=R^*-R_s^*\ \ x_1^*=\Delta p$
$f_2=h^*-h_s^*\ \ x_2^*=F_R$
$f_3=Y^*-Y_s^*\ \ x_3^*=\alpha$

where R^*, h^*, Y^*, are computed values and R_s^*, h_s^*, Y_s^* are given values at the boundary. Then the matrix $\phi\ (x^*)$ can be defined as

$$\phi\ (x^*)=\{f_{ij}(x^*)\}\quad i,j=1,2,3 \tag{21}$$

where

$$f_{ij}(x^*)=\frac{\partial f_i}{\partial x_j}(x^*) \tag{22}$$

Let x^0 be the initial starting vector. Then the computational process is to use

$$x^{*n+1}=x^{*n}-[\phi\ (x^{*n})]^{-1}\ f\ (x^{*n}) \tag{23}$$

The iteration process is repeated until the desired accuracy is achieved.

Exemplary results are presented in Fig. 2 and Table 1. Note that this bubble has a long neck and very sudden blow up which is not in quantitative agreement with experimental measurement. However, by taking thermal effects into account, we can get an improved agreement between the theoretical bubble shape and experimental measurement (Petrie [22]). The case when swelling are included was investigated by Seo and Wissler [8]. According to their results, inclusion of swelling process produces a better agreement when pulling-up ratio is low. But when pulling-up ratio is high its effect is not so apparent. This is not because of negligible swelling effect, but due to inelastic response. For Newtonian or inelastic fluids, if pulling force is strong, the swelling happens near die exit and then it vanishes very rapidly.

Improvement in comparison with experimental results was achieved when non-Newtonian fluid models were used. These require more equations for σ_{11}, σ_{22} and σ_{33} for eqn. (11) and (12). Inelastic viscous fluid equation was used by Han and Park [17] and Seo and Wissler [8]. Purely elastic models such as a rubber-like elastic or Neo-Hookean model were used in place of the Newtonian model. (Petrie [21], Wagner [24]). Difficulties were met using purely elastic models (Pearson and Gutteridge [27]). Unsatisfactory results using purely elastic models invoke the importance of the extrudate swell (Petrie [22]). To describe the viscoelastic behavior, many different constitutive equations were tried such as Leonov model (Luo and Tanner [28] and Maxwell model (Wagner [24], Luo and Tanner [28], Cao and Campbell [29]), Maxwell model expressed as a rate equation (Gupta [30]), Voigt model (Pearson and Gutteridge [27]). For viscoelastic fluids, as said above, we should have other equations to provide further informations about the stress components in the streamwise, circumferential and radial directions (for an example, see Luo and Tanner's paper [28] for Maxwell model). Also we need boundary conditions for these stress components. Numerical integration from freeze line to die, which was preferred for the Newtonian model, is highly unstable for viscoelastic fluids (Petrie [21]). As noted by Petrie, this is not really surprising since the process is an integration backwards in time for a material particle and the property of stress relaxation (for time increasing) gives exponential growth of stresses. Thus the integration should be done in the direction of increasing x. Fig. 3 shows

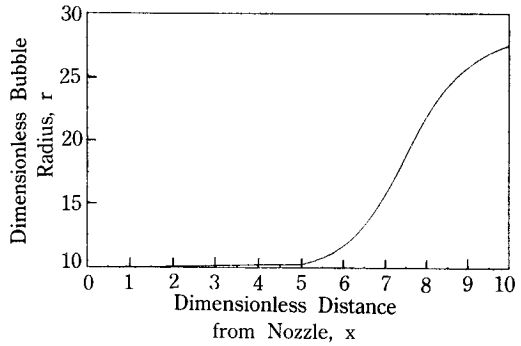

Fig. 2. A typical bubble shape for a Newtonian fluid. B=0.2, X=10, T_z=2, R=2.7 (Luo and Tanner (28)).

Table 1. Newtonian Case: results for isothermal flow (Luo and Tanner (28)

T_z	2.0	2.5	3.0
R	3.562	3.9603	4.3045
H	0.0905	0.0432	0.0189
	Case 1. B=0.15, X=6.0		
B	0.12	0.15	0.2
R	5.0186	4.3045	3.5128
H	0.0146	0.0189	0.0236
	Case 2. T_z=3.0, X=6.		
X	4.5	6.0	8.0
R	4.5447	4.3045	4.2053
H	0.0237	0.0189	0.0136
	Case 3. B=0.15, T_z=3.		

a typical result for Maxwell model and Table 2 shows some results for Maxwell model. As in the Newtonian fluid case, the bubble shape is most sensitive to B, the dimmensionless pressure difference (Table 2). The effect of λ, the relaxation time, on the behavior of the film flow is to decrease the blow-up ratio $R=A/a_0$ and to increase the thickness, since λ is an elastic or solid-like parameter. For Maxwell model, numerical results were possible only within some limited parameter values without computational instability. Fig. 4 shows a comparison of numerical results with Gupta's experiment for polystyrene film. The agreement is good. In its initial stage, blow-up ratio decreases first and then expands. This kind of necking phenomena could not be predicted with inelastic fluid models. Fig. 5 shows the comparison of circumferential stress with Gupta's experiments. Again, Maxwell model predicts the flow behaviour very well. Luo and Tanner [28] also used Leonov model. The numerical system is highly unstable when Leonov model was applied. The fluid does not stiffen enough with increasing elongational rate to simulate the bubble shape.

According to Cain and Denn's numerical results [31], Maxwell fluid shows a high draw force limit, i.e., r′ vanishes along the length of the bubble with a draw force. This happenes to both isothermal and non-isothermal case. This limit point at high draw force is an artifact of the Maxwell model, which treats polymer chains as Hookean springs that can extend indefinitely. Contrary to this inappropriate fact, network rheological models presents more realistic extensional behaviours.

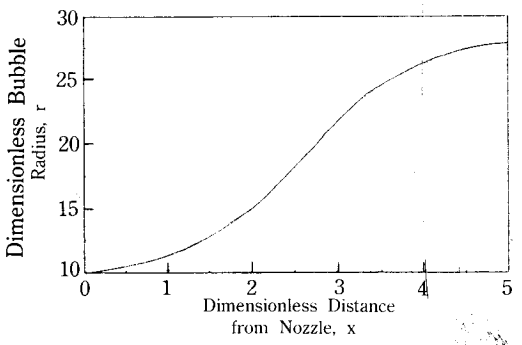

Fig. 3. A typical bubble shape for Maxwell model B=0.2, X=5, T_z=2.9, R=2.79, λ=0.15 (Luo and Tanner (28)).

Table 2. Isothermal results for Maxwell model (Luo and Tanner (28))

B	0.08	0.1
R	4.79	3.31
H	0.025	0.04
	T_z=2.8, μ=1.0, λ=1.0, X=6.0	
B	0.15	0.2
R	3.87	2.79
H	0.018	0.023
	T_z=2.9, μ=1.0, λ=0.15, X=5.0	

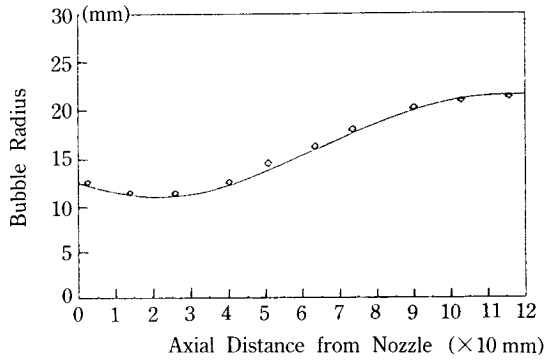

Fig. 4. Bubble shape comparison for Run 20. The ratios of theoretical to experimental values for pressure drops and axial forces respectively were 1.06 and 1.05. The line is calculated and points (◇) are expermental (Luo and Tanner (28)).

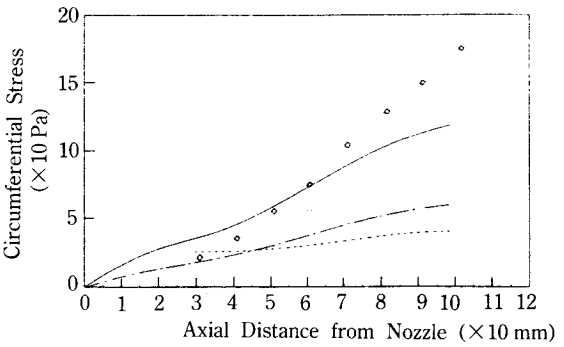

Fig. 5. Comparison of circumferential stresses for Gupta's Run 20 ···, Gupta's prediction; —·— Tanner's prediction, λ=2.93s at 170℃; —— Tanner's prediction, λ=1.173s at 170℃ (Luo and Tanner (28)).

Reflecting this idea was adopted by Cain and Denn to use Marrucci model [39]. Marucci model adds one more differential equation to the system for the structure variable. Even though comparison with experimental results is not provided, Marucci model seems good to eliminate the unstability at high draw force.

C) The Region over the Frost Line

In the film blowing process, the polymer is stretched up to the freeze line. After then the frozen strain partially relaxes as the polymer continues to cool between the freeze line and the nip rolls. Since the time it takes to cool the polymer will influence the biaxial structure developement and therefore the final physical properties of the film, it is important to extend the simulation through and above the freeze line. This approach was exploited by Cao and Campbell [29]. They expected substantial changes in structure to occur during the polymeric fluid cooling time to room temperature. Then it is easily understandable that a liquid-like model cannot be used to describe the behaviour of the film above the freeze line, since the polymer becomes solid-like. Cao and Campbell modelled film blowing process through the transition region. The material behaviour should change from liquid-like to solid-like at the frost line. They devised a mixed model which can predict the plastic-elastic transition. Including the structure memory function which has a strain hardening factor to explain the larger effective modulus in the vicinity of the freeze line, the constitutive model is cast as

$$\lambda_{eff}\overset{\triangle}{\tau}+\tau=2\eta_{eff}D \quad \text{if}\sqrt{II_r}>Y_{eff}/\sqrt{3} \tag{24}$$

$$\tau=2G_{eff}E \quad \text{if}\sqrt{II_r}>Y_{eff}/\sqrt{3} \tag{25}$$

The first one is a modified Maxwell model where $\overset{\triangle}{\tau}$ is the convective derivative as defined by Bird *et al.* [40] and the second equation is a modified Hookean model. Here

λ_{eff} = effective relation time = η_{eff}/G_{eff}
η_{eff} = effective viscosity = $\eta_f/1-(Y_{eff}/\sqrt{3})/\sqrt{II_r}$
where η_f is the fluid viscosity
Y_{eff} = effective yield stress = $Y\zeta$
Y = conventional yield stress from the Vohn-Mises yield condition (Sawer and Pae [41])
ζ = structre memory function (see Cao and Campbell)
II_r = the second invariant of deformation rate tensor
G_{eff} = effective modulus = $G(1+\zeta)$

The problem is divided into two regions, below the PET (Plastic-Elastic Transition) and above the PET. At the PET, the constitutive model shifts from the liquid-like to solid-like and the elastic strain components are obtained from it. Above the PET, since the change of angle is expected to be very small due to high effective modulus, $\theta=0$ which simplifies goverining equations as algebraic equations except the energy equation. Temperature at the plastic transition point can be used as the boundary condition. Cao and Campbell's comparison of numerical prediction with Gupta's experimental result is presented in Fig. 6 for bubble radius and Fig. 7 for the velocity. Fig. 8 shows predicted film thickness variation. When the yield stress is set to zero, the film thickness approaches zero while the velocity increases almost unbounded. This shows the importance of yield stress in the simulation. The influence of yield stress on the film velocity through effective viscosity appears to cause the film velocity to approach a limit

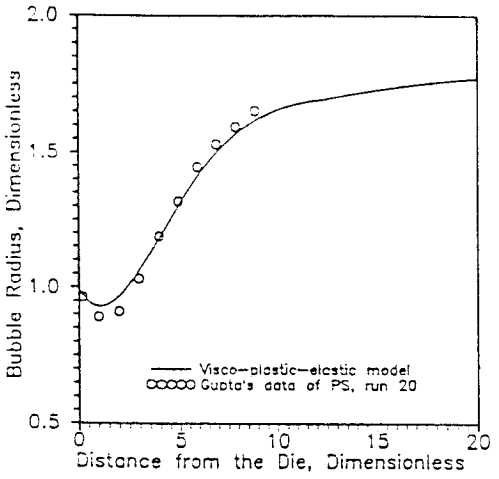

Fig. 6. Predicted bubble radius (Cao and Campbell (29)).

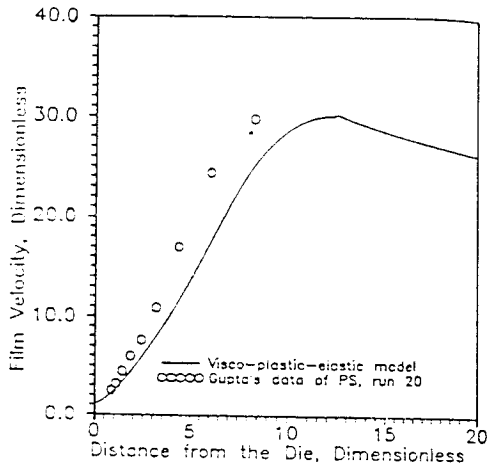

Fig. 7. Predicted film velocity (Cao and Campbell (29)).

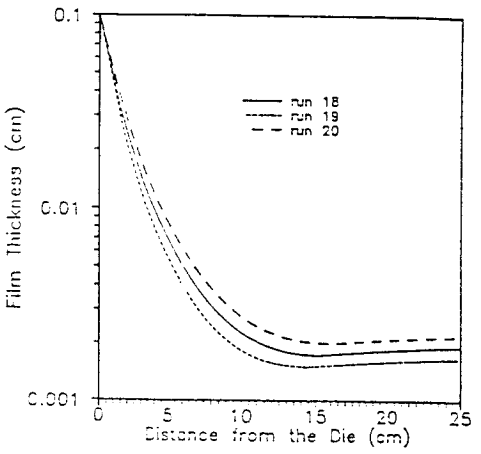

Fig. 8. Predicted film thickness (Cao and Campbell (29)).

as the effective yield stress increase due to the decreasing temperature and increasing orientation.

Stabilities in Film Blowing Process Simulation

The stabilities in film blowing process simulation were studied by many researchers experimentally and theoretically. Han and Park [17], Kanai and White [32], White *et al.* [33, 34] have reported observations of flow instabilities in film blowing experiments. Yeow [23] and Cain [35] numerically investigated bubble stability to infinitesimal disturbance. Yeow considered only Newtonian fludis, while Cain investigated both Newtonian fluid and Maxwell fluid. According to Cain's study, multiple solutions for the bubble shape are possible for some values of operating parameters, and axisymmetric steady state solutions can cease to exist in spite of small changes in operating parameters. Several types of process instabilities exist, partly depending on the selection of operating variables; one of such instability is a periodic thickness fluctuation that is analogous to draw resonance in fiber spinning. Cain solved differential equations not using previously used "shooting method" but using Newman's banded matrix technique which provides readily attainalbe solutions

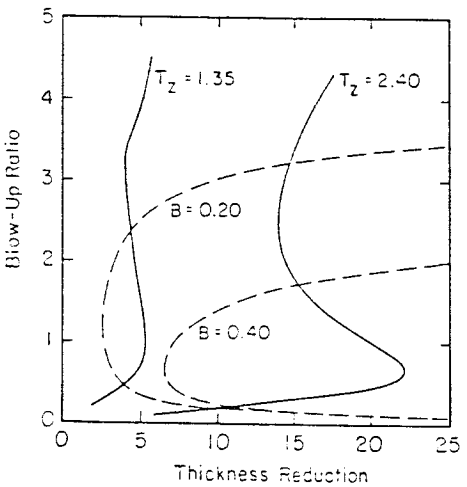

Fig. 9. Computed results for the isothermal film blowing of a Newtonian fluid, X=5 (Cain and Denn (31)).

but couldn't be obtained if shooting method was used.

Fig. 9 shows an exemplary case obtained by Cain. Several interesting features are immediately apparent. First a given draw force contour may intersect a given pressure contour more than once. So, simply defining B and T_z does not uniquely determine the bubble profile which means multiple solution can exist. Furthermore, given operating parameter contours may have no steady state solutions. The effect of the operating para-

meters variation depends upon whether the initial bubble profile is corresponding to an upper solution or a low solution. As an example, while increasing pressure from a low solutoin causes blow-up and thining, increasing from an upper solution casues draw-down and thinning. This reduction in bubble radius with increasing pressure might be sounded strangely. However, the pressure difference at starting moment reaches steady state soon. Considering larger bubble has a lower surface tension, small pressure difference is appropriate to satisfy the force balance. Hence, even though the larger initial pressure difference at the operation starting moment would be necessary, it would be smaller after it reaches the steady state. This was earlier notified by Petrie [22]. Nonisothermal Newtonian fluid behaves similarly.

For Maxwell fluids, elasticity shows different behaviour from a Newtonian fluid with increasing pressure. As pressure increases, a maximum in BUR (blow-up ratio) develops along the lower branch and a minimum along the upper branch as shown in Fig. 10. So no steady solutions can exist between the first multiple solution and the second multiple solution. There exists a branch at all pressure that ends at a point on BUR=1, corresponding to $T_2 \approx \infty$. This limit point at high draw force is an artifact of the Maxwell model, which treats

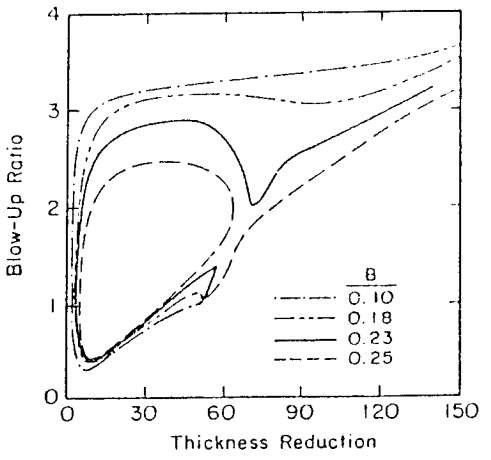

Fig. 10. Illustration of the transition from single-to double-branched pressure contours for Maxwell fluids (Cain and Denn (31)).

polymer chains as Hookean springs that can be extended indefinitely. To cure this problem, Cain used a network rheological models showing more realistic extensional behavior. The result shows a constant bubble at BUR=1. This final bubble thickness continues to decrease without bound as draw force is increased.

Cain also analyzed bubble stability to infinitesimal disturbance. Using a linear stability theory (Denn [36]), homogeneous equations with disturbance variables can be chaneged as an eigen value problem. If any eigen value of the system has a positive value, the solution is unstable to infinitesimal disturbance, since the disturbance will grow with time. Disturbance occured by variation of operating conditions (pressure, take up tension, take up velocity, and inflating air) were also investigated by Cain. The oscillatory instability can be catastrophic with positive real value. Draw resonance can happen with oscillatory instability. Increasing fluid elasticity stabilizes the process. For a Maxwell fluid, however, draw resonance still occurs with the inclusion of elasticity along the lower solution branch, but the instability is now continued within a small region and disappears as thickness reduction is further continued. Draw resonance occurred along the lower banch in weak elastic fluid was totally disappeared at the higher level of fluid elasticity. The significant stabilizing factor in film blowing process is the increase of fluid viscosity which is due to cooling. Dynamic freeze line adjustment does not eliminate draw resonance in film blowing process due to the extra degree of freedom afforded by the hoop stress balance.

Unsolved Problems in the Film Blowing Process Analysis

We just glanced over the past works of film blowing process analysis. In spite of lots of intensive works, reality is still waiting to be awaken. There are many problems we didin't or couldn't solve or approach at all. First of all, we can't, at least current moment, slove highly elastic fluid extrudate swell problem. We can easily imagine

that inclusion of extrudate swell with viscoelastic fluid model can improve the simulation. Secondly, all provious investigations follow Pearson and Petrie's mechanical model originated from Alfrey's idea. This strategy only applies to a straight upward cylindrical flow. However, in real film blowing process, rotating mandrel is used to produce more uniform and better film. There we can't apply thin-shell approximation because the flow is no more in two dimensional region. Strong hoop stress plays a very improtant role in this case. The problem is not a cylindrical flow, but a helical flow. After some distance (maybe near freeze line), higher region can be analyzed using the thin-shell approximation. But lower part should be analyzed differently. The another fact that should be mentioned is, nobody considered multilayer film blowing process from the dynamics view point, though there were some basic strudies about the multilayer flow coming out from a rotating mandrel (Alfrey *et al.* [37], Han [38]). We don't have any sound basis to approach these problems yet. Still there is a long way to go. The other fact we didn't mention in this review is that double bubble process is also used to improve the film's physical properties. Recently there were some open research papers concerned about the double process (White *et al.* [42], Takashige and Kanai [43]) and its dynamics. But its dynamic analyses are the same as single bubble process, so we don't treat them separately.

References

1. Y. Seo and K.U. Kim, *Polymer* (Korea) **13**, 10, 831 (1989).
2. M.J. Crochet, D.R. Davies and K. Walters (1984) *Numerical Simulations of Non-Newtionian Flow,* Elsevier, Amsterdam.
3. Y. Seo and E.H. Wissler, *J. Appl. Polym. Sci.,* **37**, 1159 (1990).
4. Y. Seo, *J. Appl. Polym. Sci.,* **41**, 25 (1990).
5. Y. Seo, *Polym. Eng. Sci.,* **30**, 235 (1990).
6. E. Mitsoulis, *A.I. Ch. E.,* **82**, 497 (1986).
7. M.J. Crochet and R.Keunings *J. Non-Newtonian Fluid Mech.,* 7, 199 (1980).
8. Y. Seo and E.H. Wissler, *Polym. Eng. Sci.,* **39**, 722 (1989).
9. J.R.A. Pearson and C.J.S. Petrie, *J. Fluid Mech.,* **40**, 1 (1970).
10. P.L. Clegg and N.D. Huck *Plastics,* April, 114 (1961).
11. W.A. Holmes and B. Martin, *British Plastics,* April, 232 (1966).
12. W. Ast, *Kunststoffe* **63**, 427 (1973).
13. W. Ast, *Kunststoffe* **64**, 156 (1973).
14. G. Menges and W. Predohl, *Polym. Eng. Sci.,* **15**, 394 (1975).
15. L.E. Dowd, *SPE J.* **28**, 22 (1972).
16. R. Farber and J.M. Dealy, *Polym. Eng. Sci.,* **14**, 435 (1974).
17. C.D. Han and J.Y. Park, *J. Apl. Polym. Sci.,* **19**, 3257 (1975).
18. T.J. Alfrey *SPE Transactions,* April, 68 (1965).
19. J.R.A. Pearson and C.J.S. Petrie, *J. Fluid Mech.,* **42**, 609 (1970).
20. J.R.A. Pearson and C.J.A. Petrie, *Palstics and Polym.,* **38**, 185 (1970).
21. C.J.S. Petrie *Rheol. Acta.,* **12**, 92 (1973).
22. C.J.S. Petrie in *Computational Analysis of Polymer Processing Ch.,* **7**, (Ed., J.R.A. Pearson and S.M. Richardson), Applied Scinence Publications, London (1983).
23. Y.L. Yeow, *J. Fluid Mech.,* **75**, 577 (1976).
24. M.H. Wagner, Ph.D Thesis, University of Stuttgart (1976).
25. C.D. Han and J.Y. Park, *J. Appl. Polym., Sci.,* **19**, 3291 (1982).
26. R.K. Gupta and A.B. Metzner *Polym. Eng. Sci.,* **22**, No. 8, 172 (1982).
27. J.R.A. Pearson ad P.A. Gutteridge *J. Non-Newtonian Fluid Mech.,* **4**, 57 (1978).
28. X.L. Luo and R.I. Tanner *Polym. Eng. Sci.,* **25**, 620 (1985).
29. B. Cao and G.A. Campbell *A.I. Ch. E.* **36**, 420 (1990).
30. R.K. Gupta Ph.D. Thesis, University of Delaware (1980).
31. J.J. Cain and M.M. Denn *Polym. Eng. Sci.,* **28**, 1527 (1988).
32. T. Kanai and J.L. White *Polym. Eng. Sci.,* **24**, 1185 (1984).
33. W. Minoshima and J.L. White *J. Non-Newtonian Fluid Mech.,* **19**, 275 (1986).
34. H.J. Kang and J.L. White *Polym. Eng. Sci.,* **30**, 1228 (1990).

35. J.J. Cain Ph.D. Thesis University of California, Berkeley (1987).
36. M.M. Denn *Stability of Reactcion and Transport Processes,* PrenticeHall, Englewood Cliffs, New Jersey (1975).
37. J.A. Radford, T. Alfrey Jr. and W.J. Schrenk, *Polym Eng. Sci.,* **13,** No. 3, 216 (1973).
38. C.D. Han *Multiphase Flow in Polymer Processing,* Academic Press, New York (1981).
39. D. Alcierno, F.P. La Mantia, G. Marucci and G. Titomanlio, *J. Non-Newtonian Fluid Mech.,* **1**, 125 (1976).
40. R.B. Bird R.C. Armstrong, O. Hassager, *Dynamics of Polymeric Liquids* Vol. I, Wiley, New York (1986).
41. J.A. Sauer and K.D. Pae in *Introduction to Polymer Science and Technology* Chap. 7, p.350 (Eds. H. Kaufman and J. Falcetta) Wiley, New York (1977).
42. H.J. Kang, J.L. White and M. Cakmak *Int. Polym. Proc.* **5**, 62 (1990).
43. M. Takashige and T. Kanai *Int. Polym. Proc.,* **5**, 287 (1990).

저자약력

서용석

1977 서울대학교 공업화학과 (B.S.)
1984 Univ. Texas at Austin (M.S.)
1987 Univ. Texas at Austin(Ph.D)
1989 Post Doctoral Research Fellow
Univ. Texas at Austin
1989~현재 한국과학기술연구원(KIST)
선임연구원

김광웅

1966 서울대학교 화학공학과 (B.S.)
1972 Polytechnic University(Ph.D)
1973~ Rohm and Hass Co.
Senior Scientist and Engineer
1979~1990 한국과학기술연구원(KIST)
고분자공정연구실장
1990~현재 과학기술처 화공연구조정관